# In Utero Exposure to Maternal Diabetes Impairs Vascular Expression of Prostacyclin Receptor in Rat Offspring

Jean-Paul Duong Van Huyen,[1,2] Emilie Vessières,[3] Claudine Perret,[1] Adrien Troise,[1] Sonia Prince,[1] Anne-Laure Guihot,[3] Pascal Barbry,[4] Daniel Henrion,[3] Patrick Bruneval,[1,2] Stéphane Laurent,[1,2] Martine Lelièvre-Pégorier,[1] and Céline Fassot[1]

**OBJECTIVE**—To evaluate modifications of arterial structure, gene expression, and function in our model of rats exposed to maternal diabetes.

**RESEARCH DESIGN AND METHODS**—Morphometric analyses of elastic vessels structure and determination of thoracic aortic gene expression profile with oligonucleotide chips (Agilent, G4130, 22k) were performed before the onset of established hypertension (3 months).

**RESULTS**—Arterial parameters of in situ fixed thoracic aorta were not significantly different between control mother offspring and diabetic mother offspring (DMO). The aortic gene expression profile of DMO is characterized by modifications of several members of the arachidonic acid metabolism including a twofold underexpression of prostacyclin receptor, which could contribute to decreased vasodilatation. This was confirmed by ex vivo experiments on isolated aortic rings. Pharmacological studies on conscious rats showed that systolic blood pressure decline in response to a $PGI_2$ analog was impaired in DMO rats.

**CONCLUSIONS**—These results suggest an abnormal vascular fetal programming of prostacyclin receptor in rats exposed in utero to maternal hyperglycemia that is associated with impaired vasodilatation and may be involved in the pathophysiology of hypertension in this model. *Diabetes* 59:2597–2602, 2010

Cardiovascular disease is one of the greatest health burdens worldwide. Cardiovascular risk is determined not only by conventional risk factors in adult life but also by early life events resulting in resetting of key physiological functions. Modifications of the intrauterine environment during specific windows of fetal development are now recognized as important causes of fetal stress (1), leading to several responses such as loss of structure/function and preemptive adaptations to an adverse postnatal environment (2), and finally to adult diseases such as metabolic abnormalities and hypertension (1,3).

Nutrition is one of the major intrauterine environmental factor that alters expression of the fetal genome and may have lifelong consequences leading to limited physiological function and disease (4,5). Particularly, the consequences of maternal diabetes in the adult offspring are gaining attention (6,7). Interestingly, both metabolic disorders and raised blood pressure have increasingly been associated with in utero exposure to maternal diabetes (8).

Several animal models such as modification of maternal nutrition, reduction of uterine supply, or glucocorticoid treatment have contributed to the understanding of some of the mechanisms involved in fetal/perinatal programming by showing that kidney changes and alterations of hormones regulation are involved in the fetal programming of hypertension (3,9,10). More recently, alterations of vascular function in several models of fetal programming also have been implied (11,12). In previous works (13,14), we developed a rat streptozotocin-induced model of fetal exposure to maternal diabetes, characterized by moderate levels of maternal hyperglycemia, normal gestation, and delivery with healthy pups without intrauterine growth retardation. Diabetic mother offspring (DMO) presented an established hypertension at 6 months of age (9). The exact mechanism leading to late onset of hypertension in this model is unknown. The present work was designed to evaluate changes in vascular properties through genetic profile and pharmacological studies in DMO compared with control mother offspring (CMO) at prehypertensive stage.

## RESEARCH DESIGN AND METHODS

Diabetes was induced in Sprague-Dawley rats (250–300 g) at day 0 of gestation by using a single intraperitoneal injection of streptozotocin (Sigma, 35 mg/kg) as previously described (9,13,14). The diabetic state was checked in fasted rats by measuring the plasma glucose concentration (Accuchek, Roche) on tail blood. Only pregnant females whose plasma glucose ranged between 15 and 20 mmol/l were included in the study. This diabetic status was confirmed every 2 days until delivery. On the day of delivery, the newborn rats were weished. Each litter was then reduced to 10 pups. All the animals were house kept at Centre d'Explorations Fonctionnelles. They were maintained in a temperature- and light-controlled room at 21°C with a 12-h light cycle. They had free access to food (SAFE Laboratory) and tap water. All experiments were performed at 3 months of age corresponding to prehypertensive stage. Six to seven different litters of CMO and DMO animals were used for the entire study. Each experiment was performed on males obtained from a minimum of three different litters. All experiments were conducted in accordance with the institutional guidelines and the recommendations for the care and use of laboratory animals put forward by the French Ministry of Agriculture.

**Blood pressure measurements.** Blood pressure measurements were performed on CMO and DMO animals at 3 and 12 months of age, respectively, to confirm the development of hypertension. Rats were instrumented under sodium pentobarbital anesthesia (60 mg/kg i.p.; Sanofi) with an arterial

catheter (PE-50 fused to PE-10: internal diameter, −0.28 mm; outside diameter, 0.61 mm) inserted via the femoral artery to record blood pressure. The catheter was led subcutaneously to exit between the scapulae. Upon regaining consciousness, animals were housed in individual cages. After 3 days of recovery, blood pressure was recorded on conscious unrestrained animals during 30 min. The arterial catheter was connected to a pressure transducer (P10EZ, Becton Dickinson) linked with a Gould RS 3400 polygraph to measure continuously pulsatile blood pressure.

**Histomorphometry analysis.** Morphological studies were performed on the thoracic aorta of 3-month-old CMO and DMO animals. Arterial samples were fixed in 10% buffered formalin and embedded in paraffin. Sections (6 μm) were stained with orcein for elastic fibers and sirius red for collagen to measure internal and external media perimeters, intima-media thickness, medial cross-sectional area, and elastic fiber and collagen densities of the media by computer-directed color analysis (NIS-Elements AR2.3, Nikon). Briefly, collagen and elastin densities are the ratio of the areas of collagen and elastin (stained with sirius red and orcein, respectively) detected and measured with the camera and the program-driven computer on the area of the tissue in a given microscopic field.

**Microarray analysis.** Gene expression profile was performed on thoracic aorta in 3-month-old CMO and DMO animals.

**RNA extraction of total RNA and preparation of cDNA.** Total RNA was extracted from thoracic aortic samples by TRIzol reagent (Invitrogen). The quality and concentration were checked by the Agilent technology. Good-quality RNA was amplified by the Amino Allyl MessageAmp aRNA kit (Applied Biosystems), according to the manufacturer's instructions. Ten samples (five CMO and five DMO) were isolated with sufficient yield and integrity for complete microarray analysis.

**Hybridization on microarrays.** Transcript profiling was performed using rat Agilent G4130A arrays. These microarrays contained ∼22,000 distinct oligonucleotide probes (60 mers). The list of the 22,575 probes is available online (http://www.chem.agilent.com). Antisense RNA was coupled with Cy3 and Cy5 postlabeling reactive dyes (Amersham) by a reverse transcription step. After a postprocessing step, microarrays were hybridized with labeled RNA as previously described (15). Slides were scanned with a ScanArray 5000 (GSI Lumonics), and images were quantified with the GenePix Pro 5.0 program (Axon Instruments,). This technique offers the possibility to hybridize two samples on the same slide: a control and a pathological sample. Values of pathological samples were normalized to values of control samples to compare pathological samples between them. Moreover, because incorporations of Cy3 and Cy5 dyes can differ significantly, data were further normalized using a dye-swap method (16); this method required duplication of experiments. For that purpose, a first microarray was hybridized with pathological and control samples labeled with Cy3 and Cy5, respectively. A second "swap" microarray was hybridized with pathological and control samples labeled with inverted dyes. Statistical analysis was performed using SAM software (Significance Analysis of Microarray) as described in Fig. 1. The microarray result has been deposited in the GEO database (http://www.ncbi.nlm.nih.gov/geo/) under GEO Series Accession number GSE16750.

**Confirmation of modifications observed in arachidonic acid metabolism.** Reverse transcription from 2 μg of total RNA was carried out to generate cDNA. Real-time PCR was then performed for each cDNA preparation from thoracic aorta of 3-month-old rats, using the Applied Biosystem together with the SYBRGreen master mixture for prostacyclin receptor (IP) or with the TaqMan technology for Cyp4f2. Expressions were normalized to the expression level of β-actin.

Western blot analysis of proteins of interest was performed following previously described techniques (17). Briefly, proteins were extracted from arterial biopsies of CMO and DMO. Total protein content was determined by the Bradford technique (18), and equal amounts (50 μg) of the denatured proteins were used. Membranes were incubated with polyclonal antibodies directed against IP and Cyp4f2. The detection was performed by chemiluminescence emitted from luminol oxidized by peroxidase (ECL system, Amersham).

**Pharmacological studies.** To validate functional effect of decrease in IP in DMO, we studied the effect of an analog of prostacyclin ($PGI_2$) on vascular dilatory function in isolated thoracic aorta and on blood pressure in conscious CMO and DMO animals at 3 months of age.

**Ex vivo study.** Vascular dilatory function was assessed in response to beraprost (Cayman) in isolated thoracic aorta obtained from 7 CMO and 10 DMO animals. Arterial segments (2 mm long) were dissected and mounted on a wire myograph (Danish MyoTechnology, DMT) as previously described (19). Briefly, two tungsten wires (25 μm in diameter) were inserted into the lumen of the arteries and fixed to a force transducer and a micrometer, respectively. Arteries were bathed in a 5-ml organ bath containing a physiological salt solution maintained at a pH of 7.4, a $pO_2$ of 160 mmHg, and a $pCO_2$ of 37 mmHg. After wall-tension normalization, arteries were allowed to stabilize for
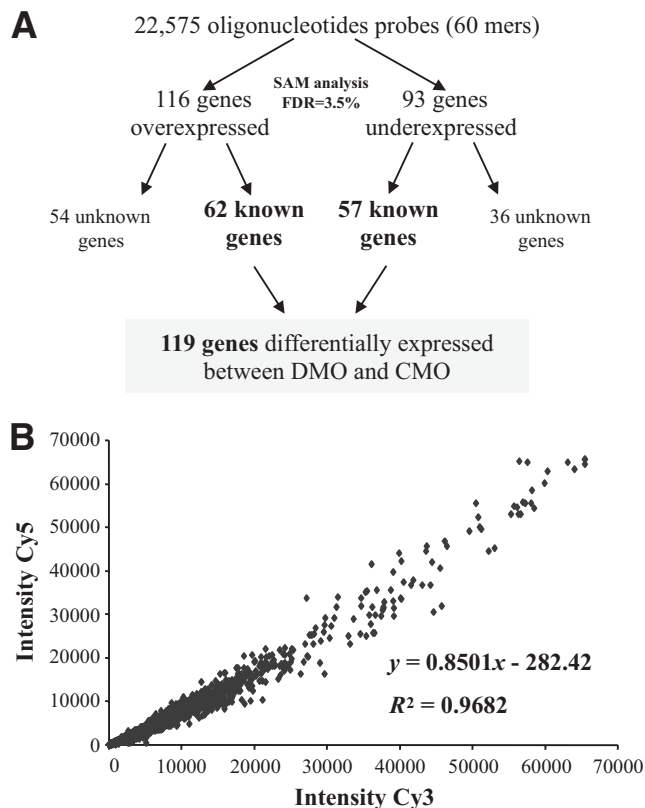


**FIG. 1. Analysis of profiling data. Scheme for analysis of profiling data at 3 months of age (*A*) and demonstration of the robustness of microarray technology with the swap method (*B*). Correlation between Cy3 values and Cy5 values obtained with the corresponding swap slide for the 22,575 transcripts. FDR, false discovery rate.**

1 h. Endothelial integrity was assessed by evaluating the vasodilator effect of $10^{-6}$ mol/l acetylcholine (Sigma-Aldrich), after preconstriction treatment with $10^{-6}$ mol/l phenylephrine (Sigma-Aldrich). Cumulative concentration–response curve to beraprost (0.001–30 μmol/l) was performed after phenylephrine-induced preconstriction (1 μmol/l). Endothelium-independent relaxation to sodium nitroprusside was obtained at the end of the protocol.

**In vivo study.** Eight CMO and six DMO animals were instrumented as described above with a supplementary venous catheter inserted into the right jugular vein to allow the injection of the pharmacological product, and the two catheters were led subcutaneously to exit between the scapulae. Systolic blood pressure (SBP) was extracted from the whole blood pressure signal, and heart rate was calculated. Recordings were performed at rest during 30 min. The experiment started when cardiovascular parameters were stable. The effect of another analog of $PGI_2$, iloprost (Schering, i.v.), was determined on arterial blood pressure and heart rate.

**Statistical analysis.** For microarray analysis, SAM (Stanford University, CA) was applied to identify genes differentially expressed between DMO and CMO. Briefly, SAM computes a score for each gene that measures the strength of transcript correlation with survival. This score (*d*) is the maximum-likelihood score statistic from Cox's proportional hazards model (Cox score). A threshold value was chosen to give a reasonably low false-positive rate (<10%), as estimated by repeatedly permuting the survival times and counting the number of genes that were significant at each threshold. Missing data were handled using the K-nearest neighbors imputer (*k* = 10) of the SAM imputation engine.

For other experiments, all results are expressed as the mean ± SEM. Statistical analysis was performed by a nonparametric Mann-Whitney test or by ANOVA when appropriate. Statistical significance was defined as $P < 0.05$.

## RESULTS

**Development of hypertension.** DMO and CMO animals had similar SBP at 3 months of age (141.9 ± 3.2 mmHg, $n = 17$, vs. 136.9 ± 3.6 mmHg, $n = 16$). SBP was significantly higher in DMO than in CMO animals at 12 months of age (166.9 ± 8.4 mmHg, $n = 8$, vs. 136.6 ± 4.5

TABLE 1
Histomorphological parameters of the thoracic aorta in 3-month-old CMO and DMO animals

| Component/parameters | CMO | DMO |
|---|---|---|
| MCSA (mm$^2 \times 10^{-3}$) | 483 ± 22 | 461 ± 11 |
| IMT (μm) | 97.1 ± 3.6 | 92.8 ± 2.3 |
| Internal perimeter (μm) | 4,921.1 ± 134.0 | 4,835.0 ± 44.8 |
| External perimeter (μm) | 5,739.3 ± 123.2 | 5,603.2 ± 29.4 |
| Elastin density (%) | 22.3 ± 0.06 | 20.0 ± 0.10 |
| Collagen density (%) | 17.6 ± 0.03 | 15.2 ± 0.02 |

Data are means ± SE. $n = 6$. IMT, intima-media thickness; MCSA, medial cross-sectional area.

mmHg, $n = 10$, $P < 0.01$). SBP increased significantly in DMO between 3 and 12 months of age ($P < 0.01$).
**Vascular structure.** Table 1 shows that arterial parameters of in situ fixed thoracic aorta were not significantly different between CMO and DMO at 3 months of age. Under light microscopy, orcein stain did not reveal morphological changes of the elastic bundles in DMO compared with CMO (data not shown).
**Microarrays analysis.** RNA samples of 3-month-old aorta were analyzed. We isolated 119 genes differentially expressed between DMO and CMO (Fig. 1$A$); the full list of these 119 genes is presented in supplementary Table 2,

available in an online appendix at http://diabetes.diabetesjournals.org/cgi/content/full/db10-0311/DC1.
Transcriptome analysis is often criticized for a lack of reproducibility of quantification. However, the requirement of duplication of experiments (use of swap) has improved this reproducibility of quantification. The specific signal associated with a *spot* (representative of a gene) was defined by the geometrical average of the specific intensities of this *spot* in direct and swapped experiments. We found a very good correlation between the intensity of a spot in direct experiment and that in swapped experiment (Fig. 1$B$).
We classified the 119 transcripts differentially expressed between groups, according to the seven functional categories described by Hwang et al. (20). As a group, transcripts encoding proteins potentially involved in the mechanical regulation of vascular function ("signaling/communication" and "structure/motility") constituted the most important group with 35% of the annotated transcripts (Fig. 2$A$). Examples of the former groups are genes related to extracellular matrix, cytoskeleton, or cellular junctions (Fig. 2$B$). Interestingly, most differentially expressed genes were implicated in the arachidonic acid metabolism. Among these genes, IP (i.e., D28966) expression was strongly reduced ($d = -1.990$, fold change = 0.5). Genes implicated in production of 20-hydroxyeicosa-
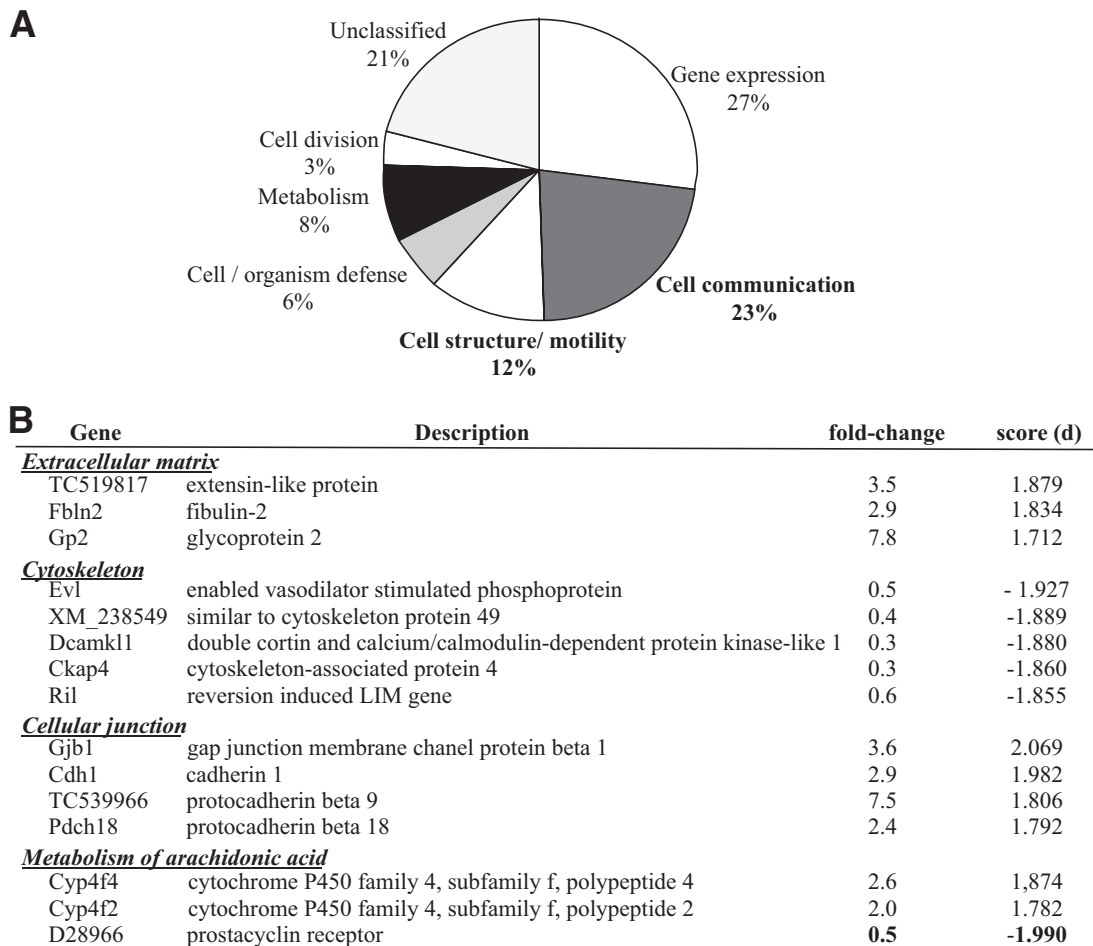


A: 
Unclassified 21%
Gene expression 27%
Cell division 3%
Metabolism 8%
Cell / organism defense 6%
Cell structure/ motility 12%
Cell communication 23%

B:

| Gene | Description | fold-change | score (d) |
|---|---|---|---|
| *Extracellular matrix* | | | |
| TC519817 | extensin-like protein | 3.5 | 1.879 |
| Fbln2 | fibulin-2 | 2.9 | 1.834 |
| Gp2 | glycoprotein 2 | 7.8 | 1.712 |
| *Cytoskeleton* | | | |
| Evl | enabled vasodilator stimulated phosphoprotein | 0.5 | - 1.927 |
| XM_238549 | similar to cytoskeleton protein 49 | 0.4 | -1.889 |
| Dcamkl1 | double cortin and calcium/calmodulin-dependent protein kinase-like 1 | 0.3 | -1.880 |
| Ckap4 | cytoskeleton-associated protein 4 | 0.3 | -1.860 |
| Ril | reversion induced LIM gene | 0.6 | -1.855 |
| *Cellular junction* | | | |
| Gjb1 | gap junction membrane chanel protein beta 1 | 3.6 | 2.069 |
| Cdh1 | cadherin 1 | 2.9 | 1.982 |
| TC539966 | protocadherin beta 9 | 7.5 | 1.806 |
| Pdch18 | protocadherin beta 18 | 2.4 | 1.792 |
| *Metabolism of arachidonic acid* | | | |
| Cyp4f4 | cytochrome P450 family 4, subfamily f, polypeptide 4 | 2.6 | 1,874 |
| Cyp4f2 | cytochrome P450 family 4, subfamily f, polypeptide 2 | 2.0 | 1.782 |
| D28966 | prostacyclin receptor | **0.5** | **-1.990** |

FIG. 2. Microarray analysis. *A*: Classification of the differentially expressed genes between DMO and CMO according to the seven functional categories described by Hwang et al. (20) at 3 months of age. *B*: Genes of interest implicated in extracellular matrix, cytoskeleton, cellular junctions, and metabolism of arachidonic acid ($d$ = statistical score).

## A



## B
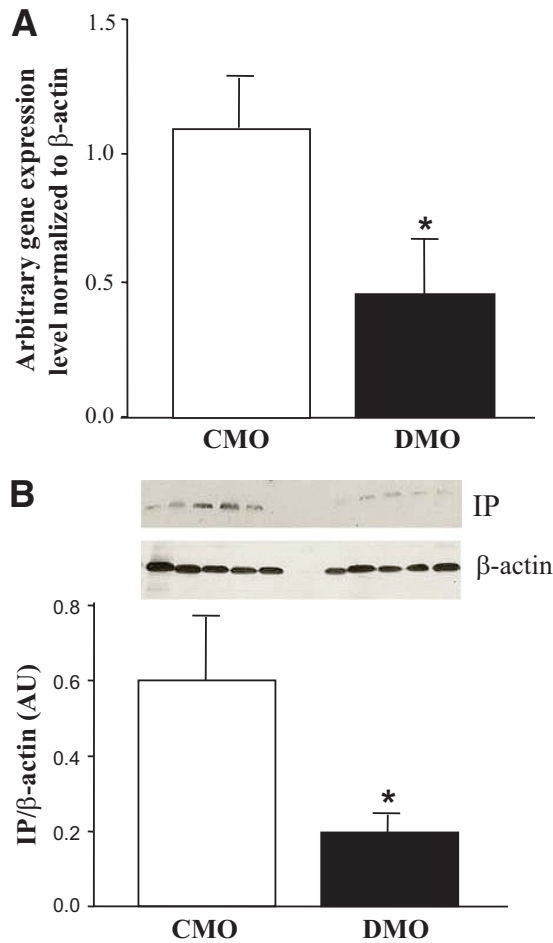


FIG. 3. Confirmation of modifications observed in arachidonic acid metabolism. *A*: Relative gene expression of IP receptor and in DMO (□, *n* = 7 from four litters) and CMO (■, *n* = 10 from four litters). *B*: Western blot analysis of IP receptor levels in the thoracic aorta of 3-month-old DMO and CMO animals. Each line corresponds to one animal from different litters. Values are means ± SEM. *$P$ < 0.01 vs. CMO.

tetraenoic acid, a potent vasoconstrictor (i.e., Cyp4f2, Cyp4f4) were overexpressed (Fig. 2*B*). These genes have the most significant *d* value correlated to the better fold change and are then considered as major targets. Modifications induced by modulation of expression of these genes involved in vascular biology could contribute to hypertension development. Thus, the following study focused on IP and Cyp4f2.

**RT-PCR and protein analysis.** RT-PCR and Western blot analysis were performed on CMO and DMO thoracic aorta in another independent experimental set of rats to confirm the modulation of expression of IP and Cyp4f2 genes. A significant downregulation was detected in the IP gene in DMO compared with CMO. Relative gene expression levels were 0.46 ± 0.22 in DMO and 1.10 ± 0.24 in CMO (respectively, *n* = 7 and *n* = 10, each from four different litters, $P$ < 0.05, Fig. 3*A*). The decreased expression of IP transcript was confirmed at the protein level (*n* = 5 from three different litters, Fig. 3*B*), with an ~2.5-fold decrease in DMO compared with CMO ($P$ = 0.048), consistent with the 0.5-fold underexpression of the corresponding gene observed by microarray and RT-PCR. We did not detect any significant increase of Cyp4f2 at gene and protein levels (data not shown).

**Pharmacological studies.** We examined whether the decrease in IP protein level was associated with functional
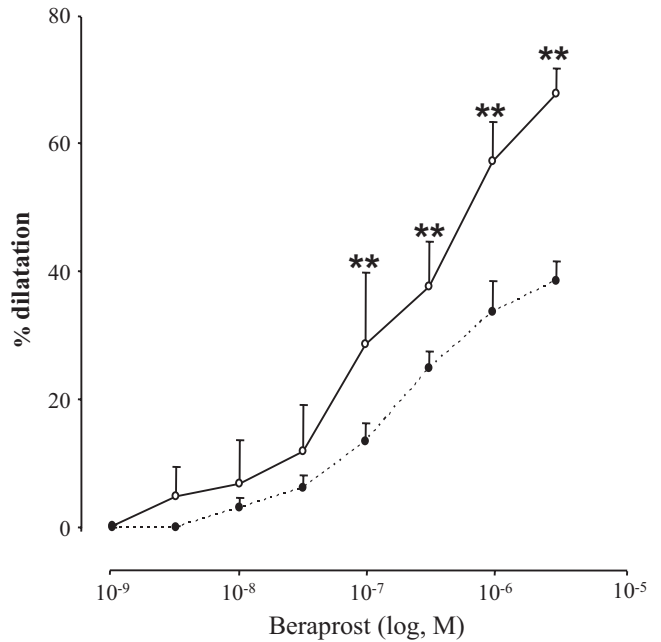


FIG. 4. Changes in diameter in response to beraprost mediating vasodilatation in thoracic aortic rings of CMO (○, *n* = 7) and DMO (●, *n* = 10) at 3 months of age. Values are means ± SEM. **$P$ < 0.01 vs. CMO.

modifications. Ex vivo experiments on isolated thoracic aorta rings showed a significantly decreased vasodilatory function in DMO compared with CMO (Fig. 4, $P$ < 0.01) in response to beraprost.

During in vivo experiments, we observed a blunted decrease in SBP in response to 4 ng/kg/ml iloprost in DMO (−10.7%, from 139 to 124 mmHg) compared with CMO (−24.1%, from 134.4 to 105.8 mmHg, $P$ = 0.040, for difference, Fig. 5), whereas SBP was identical at lower dosage. Heart rate was similar in the two groups (377.0 ± 10.9 bpm in DMO vs. 371.5 ± 12.6 bpm in CMO) at any dose.

### DISCUSSION

The major result of the present study is that exposure to maternal diabetes is associated with profound changes in aortic gene expression and function in the adult offspring.
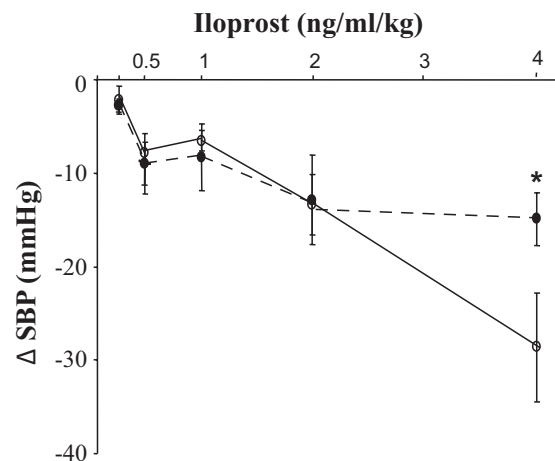


FIG. 5. Pharmacological studies. Dose-response curve to iloprost in CMO (○) and DMO (●). Values are means ± SEM. *$P$ < 0.05 vs. CMO.

Indeed, we identified a specific gene expression profile of the thoracic aorta in DMO rats, including genes related to extracellular matrix, cytoskeleton, or cellular junctions and arachidonic acid metabolism. We focused on members of the arachidonic acid metabolism and found that IP expression was reduced by 50% at the messenger and protein levels in aorta of the DMO rats. Functional implication of IP downexpression was demonstrated in aortic ring experiments with an impaired vasodilatation response to $PGI_2$ analog of vessels issued from DMO rats. Concurrently, in vivo experiments showed that $PGI_2$ analog-dependent effect on SBP was blunted in DMO.

Our experimental study showing a reduced vascular expression of IP in animals exposed in utero to maternal diabetes reinforces the evidence of a reprogramming of vascular function by modifications of the intrauterine environment. Indeed, vascular functions in the rat offspring have been recently investigated in models of impairment of maternal diet during pregnancy, that is, high-fat, hypocaloric, or low-protein diets. These studies have evidenced a vascular dysfunction mainly related to impaired endothelial functions through the assessment of the NO pathway (11,12,21,22). One must note that, in contrast to our experimental protocol, several of these works were conducted in established hypertension and thus did not address early abnormalities of the vessel wall. Thus, it is still unclear whether these abnormalities, that is, impaired endothelium-dependent relaxation, occur first or develop as a consequence of hypertension. However, endothelial dysfunction may occur without hypertension; Rodford et al. (23) recently identified reduced endothelial responsiveness to acetylcholine, unexpected increased eNOS vascular expression, and systemic reduction of antioxidant protection in a protein-restricted rat model with normal blood pressure. Concerning exposure to maternal diabetes, Rocha et al. (24) showed a decreased endothelium-dependent vasodilatation in mesenteric arteries of 12-month-old rats (after several months of hypertension) issued from diabetic mothers.

Vascular fetal programming of $PGI_2$/IP pathway has never been reported until now. Because prostacyclin plays a key role in several vascular functions, in particular in the control of vascular tone by promoting vasodilatation and differentiation of vascular smooth muscle cell (25), our results raise the question of the consequences of an early downexpression of vascular IP (3-month-old animals) in view of the hypertension that will be established at 6 months in our model. First, prostacyclin analog was less effective in reducing blood pressure in DMO rats as compared with CMO. This indicates that IP downexpression is involved in the abnormal regulation of blood pressure in DMO. Second, at the vascular level, although vasodilatation properties of resistance arteries, that is, mesenteric arteries, are not evaluated here, impaired vasodilatation response to $PGI_2$ analog is evidenced in DMO aortic rings. Together, these results suggest that IP-decreased expression may participate in abnormal regulation of arterial pressure in DMO through impaired vasodilatation responses. Interestingly, vascular expression of IP- has been studied in spontaneous hypertensive rats (SHR). In this strain, Numaguchi et al. (26) showed a diminished expression of IP mRNA in thoracic aorta before the onset of hypertension (1 month of age). However, in established hypertension (9 months of age), Tang and Vanhoutte (27) showed similar levels of IP transcripts in vascular smooth muscle cells of SHR compared to Wistar Kyoto. At a functional level, relaxation obtained in aortic rings, in response to $PGI_2$ or IP agonist, was impaired in 3-month-old SHR and was further decreased in older animals (28).

To conclude, our experimental study shows that exposure to maternal diabetes is associated with a decreased IP vascular expression in the adult offspring. Although it is not currently known if fetal programming of IP may be relevant in humans, a recent study on a natural mutation of IP (R212C variant, defective in adenyl cyclase activation) has shown that impaired $PGI_2$ signaling appears to contribute to the cardiovascular phenotype in a risk factor–dependent manner (29). If applicable in humans, the concept of prenatal resetting of vascular functions by maternal nutrition and particularly by maternal diabetes would certainly open new epidemiologic and therapeutic perspectives.

## REFERENCES

1. Gluckman PD, Hanson MA, Cooper C, Thornburg KL. Effect of in utero and early-life conditions on adult health and disease. N Engl J Med 2008;359:61–73
2. Ingelfinger JR. Prematurity and the legacy of intrauterine stress. N Engl J Med 2007;356:2093–2095
3. McMillen IC, Robinson JS. Developmental origins of the metabolic syndrome: prediction, plasticity, and programming. Physiol Rev 2005;85:571–633
4. Wu G, Bazer FW, Cudd TA, Meininger CJ, Spencer TE. Maternal nutrition and fetal development. J Nutr 2004;134:2169–2172
5. McMullen S, Gardner DS, Langley-Evans SC. Prenatal programming of angiotensin II type 2 receptor expression in the rat. Br J Nutr 2004;91:133–140
6. Fetita LS, Sobngwi E, Serradas P, Calvo F, Gautier JF. Consequences of fetal exposure to maternal diabetes in offspring. J Clin Endocrinol Metab 2006;91:3718–3724
7. Simeoni U, Barker DJ. Offspring of diabetic pregnancy: long-term outcomes. Semin Fetal Neonatal Med 2009;14:119–124
8. Wright CS, Rifas-Shiman SL, Rich-Edwards JW, Taveras EM, Gillman MW, Oken E. Intrauterine exposure to gestational diabetes, child adiposity, and blood pressure. Am J Hypertens 2009;22:215–220
9. Nehiri T, Duong Van Huyen JP, Viltard M, Fassot C, Heudes D, Freund N, Deschênes G, Houillier P, Bruneval P, Lelièvre-Pégorier M. Exposure to maternal diabetes induces salt-sensitive hypertension and impairs renal function in adult rat offspring. Diabetes 2008;57:2167–2175
10. Vehaskari VM, Woods LL. Prenatal programming of hypertension: lessons from experimental models. J Am Soc Nephrol 2005;16:2545–2556
11. Lamireau D, Nuyt AM, Hou X, Bernier S, Beauchamp M, Gobeil F Jr, Lahaie I, Varma DR, Chemtob S. Altered vascular function in fetal programming of hypertension. Stroke 2002;33:2992–2998
12. Torrens C, Brawley L, Barker AC, Itoh S, Poston L, Hanson MA. Maternal protein restriction in the rat impairs resistance artery but not conduit artery function in pregnant offspring. J Physiol 2003;547:77–84
13. Amri K, Freund N, Duong Van Huyen JP, Merlet-Bénichou C, Lelièvre-Pégorier M. Altered nephrogenesis due to maternal diabetes is associated with increased expression of IGF-II/mannose-6-phosphate receptor in the fetal kidney. Diabetes 2001;50:1069–1075
14. Amri K, Freund N, Vilar J, Merlet-Bénichou C, Lelièvre-Pégorier M. Adverse effects of hyperglycemia on kidney development in rats: in vivo and in vitro studies. Diabetes 1999;48:2240–2245
15. Moreilhon C, Gras D, Hologne C, Bajolet O, Cottrez F, Magnone V, Merten

M, Groux H, Puchelle E, Barbry P. Live Staphylococcus aureus and bacterial soluble factors induce different transcriptional responses in human airway cells. Physiol Genomics 2005;20:244–255

16. Kerr MK, Churchill GA. Experimental design for gene expression microarrays. Biostatistics 2001;2:183–201

17. Fassot C, Briet M, Rostagno P, Barbry P, Perret C, Laude D, Boutouyrie P, Bozec E, Bruneval P, Latremouille C, Laurent S. Accelerated arterial stiffening and gene expression profile of the aorta in patients with coronary artery disease. J Hypertens 2008;26:747–757

18. Bradford MM. A rapid and sensitive method for the quantitation of microgram quantities of protein utilizing the principle of protein-dye binding. Anal Biochem 1976;72:248–254

19. Belin de Chantemèle EJ, Retailleau K, Pinaud F, Vessières E, Bocquet A, Guihot AL, Lemaire B, Domenga V, Baufreton C, Loufrani L, Joutel A, Henrion D. Notch3 is a major regulator of vascular tone in cerebral and tail resistance arteries. Arterioscler Thromb Vasc Biol 2008;28:2216–2224

20. Hwang DM, Dempsey AA, Wang RX, Rezvani M, Barrans JD, Dai KS, Wang HY, Ma H, Cukerman E, Liu YQ, Gu JR, Zhang JH, Tsui SK, Waye MM, Fung KP, Lee CY, Liew CC. A genome-based resource for molecular cardiovascular medicine: toward a compendium of cardiovascular genes. Circulation 1997;96:4146–4203

21. Franco Mdo C, Arruda RM, Dantas AP, Kawamoto EM, Fortes ZB, Scavone C, Carvalho MH, Tostes RC, Nigro D. Intrauterine undernutrition: expression and activity of the endothelial nitric oxide synthase in male and female adult offspring. Cardiovasc Res 2002;56:145–153

22. Brawley L, Itoh S, Torrens C, Barker A, Bertram C, Poston L, Hanson M. Dietary protein restriction in pregnancy induces hypertension and vascular defects in rat male offspring. Pediatr Res 2003;54:83–90

23. Rodford JL, Torrens C, Siow RC, Mann GE, Hanson MA, Clough GF. Endothelial dysfunction and reduced antioxidant protection in an animal model of the developmental origins of cardiovascular disease. J Physiol 2008;586:4709–4720

24. Rocha SO, Gomes GN, Forti AL, do Carmo Pinho Franco M, Fortes ZB, de Fátima Cavanal M, Gil FZ. Long-term effects of maternal diabetes on vascular reactivity and renal function in rat male offspring. Pediatr Res 2005;58:1274–1279

25. Fetalvero KM, Shyu M, Nomikos AP, Chiu YF, Wagner RJ, Powell RJ, Hwa J, Martin KA. The prostacyclin receptor induces human vascular smooth muscle cell differentiation via the protein kinase A pathway. Am J Physiol Heart Circ Physiol 2006;290:H1337–H1346

26. Numaguchi Y, Harada M, Osanai H, Hayashi K, Toki Y, Okumura K, Ito T, Hayakawa T. Altered gene expression of prostacyclin synthase and prostacyclin receptor in the thoracic aorta of spontaneously hypertensive rats. Cardiovasc Res 1999;41:682–688

27. Tang EH, Vanhoutte PM. Gene expression changes of prostanoid synthases in endothelial cells and prostanoid receptors in vascular smooth muscle cells caused by aging and hypertension. Physiol Genomics 2008;32:409–418

28. Gomez E, Schwendemann C, Roger S, Simonet S, Paysant J, Courchay C, Verbeuren TJ, Félétou M. Aging and prostacyclin responses in aorta and platelets from WKY and SHR rats. Am J Physiol Heart Circ Physiol 2008;295:H2198–H2211

29. Stitham J, Arehart EJ, Gleim S, Douville K, MacKenzie T, Hwa J. Arginine (CGC) codon targeting in the human prostacyclin receptor gene (PTGIR) and G-protein coupled receptors (GPCR). Gene 2007;396:180–187